

# Viscoelastic Properties for Sol-Gel Transition

Yutaka Tanaka

*University of Fukui, Dept. of Engineering,  
Japan*

## 1. Introduction

Gel formation is inseparable from viscoelastic properties. Research works of gels usually accompany viscoelastic methodology, because the gel formation closely related to the disappearance of fluidity in colloidal system, which frequently occurs in a polymer solution. (Almdal et al., 1993) Change in viscoelastic properties is significant during the gelation process of a polymer solution, where three dimensional networks coming from cross-links between chains have the key role.

The system is liquid-like and often called as sol before cross-linking starts, and remains a liquid until the viscosity becomes infinite. At that moment, called as gel point, there is at least one molecule with an infinite molecular weight. Beyond the gel point, evolution of elastic modulus follows with the progress of cross-links. As for networks, various formations can be observed, those are thermoreversible, often seen in natural polymer, irreversible, physically cross-linked, chemically cross-linked, super molecular - developed recently in advanced materials - and so on. The dramatic change in viscoelasticity is of interest from both practical and physicochemical points of view, and many research works have been carried out. Also, several reviews have been published for gels and sol - gel transition. Ross-Murphy and Clark gave a review on physical gels. (Clark & Ross-Murphy, 1987) Extensive monographs on thermoreversible gelation were produced by Guenet and Nijenhuis. (Guenet, 1992; Nijenhuis, 1997) As for the structure and properties of polymer networks, Stepto compiled research works. (Stepto, 1998)

With a consideration on these existing research results, this chapter approaches to the viscoelasticity of gelation with several topics; those are theoretical and experimental works on power laws observed for various properties in sol-gel transition region, delay of gel point and the ring formation for the gelation of  $RA_{fa} + R'B_{fb}$  type polymerisation, network formation by the end-linking of star polymer and the viscoelastic behaviour.

## 2. Evolution of viscoelasticity near sol-gel transition

### 2.1 Sol - gel transition and power law

The gelation has attracted many research workers, especially in the field of polymer science, which probably is because gels are complex systems. In fact, in the respective gels their own complexities are presented. To overcome the complexities of network structure and describe successfully the formation and properties of gels, various theoretical models have so far

been proposed. In Section 2.1.1, Bethe lattice was demonstrated as an example of plain models to express the gel point prediction. In Section 3.1, a network formation model of rather specific structure is described to account for the delay of gel point.

As for the description of gelation, the framework of scaling is frequently used to account for both experimental and theoretical research results. As is well known, power law appears for many physical parameters to capture polymer properties in the scaling law. Also in the model of Bethe lattice, quite a few power law dependences can be seen for gel fraction, degree of polymerisation etc. In Section 2.1.2, those relationships are shown to discuss the analogues between properties of gel and other physical phenomena.

Intensive research works have been carried out by Winter et al., over many years to elucidate the power law observed for the sol-gel transition, which is shown in Section 2.1.3. (Winter, 1997) The concepts of mechanical self-similarity, and further topological self-similarity as its extension, have been introduced by their studies, where the same properties are found at different length scales within the observed network. Afterwards, their research results have been accepted broadly. Many works follow to find the experimental results of various polymer gels to obey power law relaxation. With these research results, theoretical works in relation to sol-gel transition is discussed in the following three sections.

### **2.1.1 Bethe lattice, an example of percolation model to account for gelation**

It is Flory who first gave theoretical framework on the gelation. The idea starts with the generating of branching during polymerisation. The branchings take place repeatedly which eventually lead to the formation of the infinite network. (Flory, 1941) Afterwards, modified ideas have been proposed by many researchers. (Gordon & Ross-Murphy, 1975; Miller & Macosko, 1978)

Another trend towards the model of a satisfactory interpretation of the experimental data comes from physics of phase transition which regards the gelation as an example of critical phenomenon. This trend is developing with the viewpoint of scaling approaches for the static and dynamic properties of gels. The scaling concepts introduced into the theory of polymer solutions were subsequently extended to the description of swollen networks.

It is possible to consider the transition from sol to gel with the percolation model, which illustrates the process of gel formation by the linkage of two dots where many dots are spaced regularly. An example of the experimental system is the monomer sample including no solvent, where the functionality of the monomer is larger than three.

In the model, the monomers lie on the lattice points. The linkage, referred to as bond, randomly occurs only between neighbouring monomers. Let the probability of the bond formation be  $p$ , and the definition of  $s$ -cluster is given with  $s$ , the number of monomers included in the cluster. Then,  $s$ -clusters of the finite size appear at  $p < p_c$  for a given value of  $p_c$ , which corresponds with sol. For  $p > p_c$ , at least one infinite cluster and  $s$ -clusters of various sizes appear, which corresponds with gel. And consequently, sol-gel transition is the change in phase from sol comprised of  $s$ -clusters of finite size to gel having at least one infinite cluster. The probability of the bond formation is the predominant parameter whether or not the system in the lattice turns to gel. This process is called as the bond percolation.  $p_c$  of a threshold corresponds with gel point. The examples of real

experimental parameters of  $p$  are temperature, pH, concentration, the extent of reaction of the monomer, etc.

The physical quantities relating to gelation can be derived using a lattice model of Bethe lattice which is an example of percolation models. Figure 1 shows Bethe lattice where the coordination number,  $z$ , is  $z=3$ , meaning that the dot corresponds with the monomer whose functionality is equal to three; the dot is called as the site in the model. Bonds of  $z$  emanate from the site of the centre, also sites are at the opposite end of the bonds. Then, another  $z$  bonds emanate from each of these sites again; one of  $z$  bonds is tied with the site of the centre, the other  $(z - 1)$  bonds extend outwards. Accordingly, the branching takes place repeatedly in Bethe lattice.

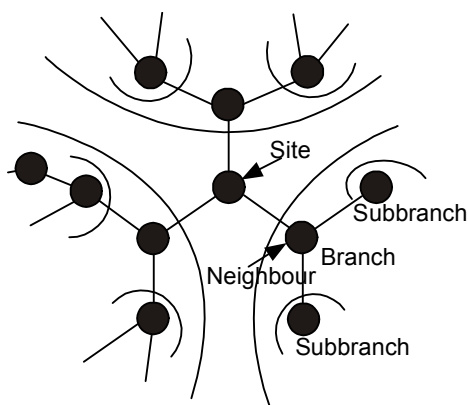


Fig. 1. The surroundings of the origin of a large Bethe lattice.

It is a remarkable feature that Bethe lattice has no closed loops. If a site was chosen randomly and moved to the neighbouring site, then new sites of  $(z - 1)$  come in. It is always new sites as long as moving forwards. The definitions of branch, neighbour, subbranch are shown in Figure 1 as they will be used later.

To define the threshold of  $p_c$  statistically, the probability of path continuation is introduced. It is the probability that a randomly chosen site has at least one path emanating from it that continues to infinity. This probability increases as the increase in  $p$ , and becomes equal to unity at  $p_c$ . Now, we will consider the path continuation from the randomly chosen site to its neighbour. There are  $(z - 1)$  sites available around the neighbour except for the first site chosen randomly; the neighbour can form a bond to each of these sites with the probability of  $p$ . Therefore, the randomly chosen site can form bonds of  $(z - 1) \times p$  with its neighbours on average. At the critical percolation point, we have  $(z - 1) \times p_c = 1$  and the gel point can be given as,

$$p_c = 1/(z - 1) \quad (1)$$

Next, the percolation probability, denoted as  $P$  is derived; that is, the probability that a randomly chosen site is in the cluster of infinite size.  $P$  corresponds with the gel fraction in the experimental system. Let the probability that the particular branch emanating from a randomly chosen site does not continue to infinity, be  $H$ .  $H$  is the sum of two cases. One is

that the bond does not form between the randomly chosen site and the branch, which probability is  $(1-p)$ . The other one is that the bond forms, but the branch does not continue to infinity, which probability is  $pH^2$ . We have, consequently,

$$H = pH^2 + (1-p) \quad (2)$$

Furthermore, the probability that the neighbour of the randomly chosen site continue to infinity is given as  $(1-H^3)$ , because  $H^3$  means there is no path to infinity from the neighbour through each of three branches. The probability of bond formation between the randomly chosen site and neighbour is  $p$ , and thus  $P = (1-H^3) \times p$  is obtained. From the solution of eq.(2), as eq.(2) is a quadratic equation of  $H$ ,  $P$  can be expressed as a function of  $p$ .

$$P = 0 \text{ for } p < p_c, P = \frac{(p-1)^3 - p^3}{p^2} \text{ for } p > p_c \quad (3)$$

Eq.(3) is equivalent with the result of the weight fraction of gel Flory derived using the branching model.(Flory, 1941)

Next, the averaged cluster size,  $S$  is derived;  $S$  corresponds with the weight average molecular weight in the experimental system. The result of the expressions of  $S$  is described here,

$$S = \frac{p(1+p)}{(1-2p)} \quad (4)$$

Using eqs. (3) and (4) the critical behaviours for  $P$  and  $S$  can be examined near the threshold of  $p_c$ . If the probability of bond formation is larger than  $p_c$  and close to  $p_c$ , then only one infinite cluster exists and  $P$  becomes small. In fact, provided that  $z=3$ , i.e.,  $p_c=(1/2)$ ,  $P=0$  at  $p=p_c$  (see the solution of eq.(2)), then we have,

$$P \propto (p - p_c).$$

As for the averaged cluster size, if  $p$  is smaller than  $p_c$  and approaches to  $p_c$ , then  $S$  increases rapidly. That is,  $S$  diverges at  $p=p_c$  (see eq.(4)), which situation corresponds to the divergence of the weight-average molecular weight at gel point for the experimental system. The equation of  $S$  near the gelation threshold is given as,

$$S \propto (p_c - p)^{-1}.$$

From the arguments regarding Bethe lattice described above, several expressions of critical behaviour can be obtained for physical parameters of sol-gel transition. Likewise, the consideration on 3-dimensional lattice will give the expressions of  $P$  and  $S$  in the form of power law. Further, more generalised formulas can be obtained for  $d$ -dimensional lattice of  $d>3$  as,

$$P \propto (p - p_c)^\beta \quad (5a)$$

$$S \propto (p - p_c)^\gamma \quad (5b)$$

Other physical parameters like number of  $s$ -cluster, radials of cluster, correlation length etc will be described in the next section.

For the gel point prediction which is applicable to the experimental data, it is necessary to introduce solvent molecules to the lattice model shown above. The introduction of solvent is the process to lay both monomer and solvent molecules randomly to lattice dots (that is, sites), which is known as the site percolation. In the lattice model, the site percolation assumes that, whenever a monomer is laid in the neighbour, the mutual bond is necessarily produced between neighbours. The probability of the site occupation by the monomer is the dominant factor of the gelation. In the experimental system, the probability of occupation corresponds with the monomer concentration. The cluster of infinite size appears above the threshold of the probability of occupation.

The site-bond percolation can be given as an extension of the site percolation, which accounts for the sol-gel transition of the systems comprised of monomer and solvent. The result of the site-bond percolation over a lattice model is shown in Figure 2, where the probability of site occupation,  $\phi$ , and that of the bond formation,  $p$  were varied independently. The prediction of sol-gel transition like Figure 2 has been compared with the experimental results for the solution of polystyrene and carbon disulfide. (Tan et al., 1983)

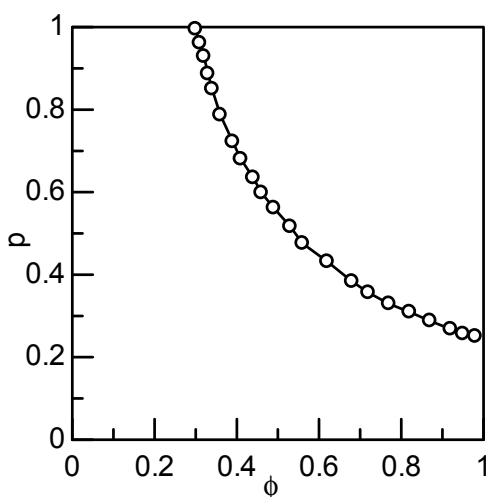


Fig. 2. Phase diagram of random site- bond percolation.

### 2.1.2 Power law near sol-gel transition

The gelation process is analogous to the percolation with some simplicities. The analogues are studied by Stauffer et al., for physical parameters appeared in the different transitions of percolation, sol-gel transition, liquid-gas transition, the ferromagnet. (Stauffer, 1981) In particular, the power law dependences of several physical parameters near the transition point were taken as the research object. Those relationships are usually in the form of power function of the relative distance from the critical point as seen below. Table 1 shows the analogies in the critical behaviour. The power laws of the gel fraction and the degree of polymerisation are already seen in eqs.(5a and 5b). Likewise, the critical exponents of physical quantities regarding sol-gel transition can be given as follows.

$$G \propto |(p - p_c)/ p_c|^\beta \quad (6)$$

$$DP_w \propto |(p - p_c)/ p_c|^{-\gamma} \quad (7)$$

$$\xi \propto |(p - p_c)/ p_c|^{-\nu} \quad (8)$$

$$E \propto |(p - p_c)/ p_c|^t \quad (9)$$

$$\eta \propto |(p - p_c)/ p_c|^k \quad (10)$$

$\eta$  is the viscosity of the solution and given in the pre-gel stage.  $E$  is the elasticity and given in the post-gel stage.

It is not until the comparison with the experimental data are made that the significance of the power law dependence, and hence the significance of the physical parameters of eqs.(6-10) are clarified. Several experimental results for the exponents of power law have been compiled by Brauner.(Brauner, 1979) The gelling substances taken up in his work were, polystyrene cross-linked with divinylbenzene, poly(vinyl chloride), poly(diallyl phthalate), deoxy hemoglobin, amylose etc. It turns out from the data compilation that values of  $\beta$ ,  $\gamma$ ,  $k$  scatter well depending on experimental systems. One of the causes of the data scattering is that the exponent is sensitive to the choice of  $p_c$  and the experimental determination of the exponent is unstable. In this regard, Gordon et al. also pointed out to be cautious on the estimation of the transition point; they examined the soluble fraction as a function of heating time for the coagulation of milk.(Gordon&Torkington, 1984) In addition, the range of the variable of  $p$  will influence on the estimation of the exponent; the exponent might be determined using  $p$  and other values in the outside of the critical behaviour. As a result, it is still a controversial issue whether the experimental values are equivalent with those predicted by percolation.

Gelation	Percolation	liquid-gas	ferromagnet
$G$ : gel fraction	$P_\infty$ : percolation probability	$\Delta\rho$ : density difference	$M_0$ : spontaneous magnetisation
$DP_w$ : degree of polymerisation	$S$ : mean size of finite cluster	$\kappa$ : compressibility	$\chi$ : susceptibility
$\xi$ : correlation length	$\xi$ : correlation length	$\xi$ : correlation length	$\xi$ : correlation length
$p_c$ : gel point	$p_c$ : percolation threshold	$T_c$ : critical temperature	$T_c$ : curie temperature
$p$ : conversion	$p$ : probability	$T$ : temperature	$T$ : temperature

Table 1. Analogies in the critical behaviour of different phase transitions.

An example of experimental determination of  $t$  value is shown in Figure 3.(Nakamura, 1993) The sample is gellan, polysaccharide, one of the gelling agents. Its aqueous solution shows thermoreversible sol-gel transition, which depends on concentration and temperature. The aqueous solution is sol at high temperature and gel at low temperature. Taking the

correspondence between the solution and the percolation, the probability of the site occupation is proportional to the concentration of gellan, the probability of the bond formation is roughly proportional to temperature. Therefore, the measurement of temperature dependence of the elasticity corresponds to the examination of bond percolation under the constant probability of the site occupation. The following equation was applied to the result of the measurement, then data were plotted in Figure 3.

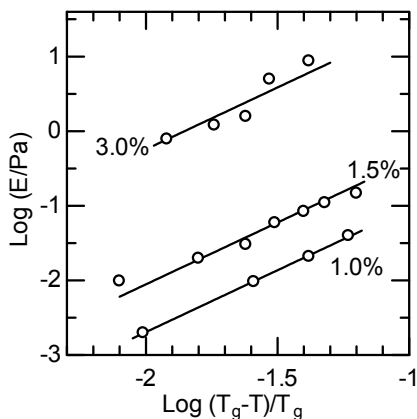


Fig. 3. Logarithmic plot of elasticity as a function of the reduced temperature for aqueous gellan solutions of 1.0%, 1.5%, 3.0%.

$$E = C \cdot \left| \frac{T_g - T}{T_g} \right|^t \quad (11)$$

$C$  is the proportional constant,  $T$  is temperature of the aqueous solution,  $T_g$  the temperature of gelation. The result shows  $t=1.5$  being independent of the concentration, which is close to the prediction of the percolation.

Some unsolved problems remain in the critical behaviour of sol-gel transition. Those are, the relations between different exponents, the exponent and molecular mechanism, and so on. Nevertheless, the applicability of power law to several physical properties, the analogy between sol-gel, liquid-gas, ferromagnet transitions, the relevance to the volume phase transition of gel (Tanaka, 2011), these matters contain research objects of much interests.

### 2.1.3 Mechanical self similarity and scale of observation

Several power functions were found between various physical quantities in relation to polymer gel. Of these power laws, the discovery of the relations for frequency and dynamic viscoelasticity of  $G'(\omega)$  and  $G''(\omega)$  has attracted much interest, and many research workers followed the frequency power law of the gelation. The application of the frequency power law to the gel point was first proposed by Winter et al. (Winter and Mour, 1997) Their experimental results suggested, at first, new methods for localising the gel point by the detection of a loss tangent independent of the frequency. Moreover, they discussed that the topological self similarity in the polymer network can be related to the straight line in  $G'(\omega)$

and  $G''(\omega)$  over wide frequencies in the double logarithmic plot, described as, (Winter, 1987; Vilgis&Winter, 1988)

$$G'(\omega) \propto \omega^p, G''(\omega) \propto \omega^p. \quad (12)$$

In their studies, dynamic mechanical experiments in small amplitude oscillatory were carried out for the end-linking polydimethylsiloxane and polyurethane. The extent of reaction,  $p$ , of the end-linking is the variable to dominate sol-gel transition. The gel point of the polydimethylsiloxane network appears at  $p=p_c$ . A simple power law was found to govern the viscoelastic behaviour of the critical gel, described by a complex modulus

$$G^*(\omega, p_c) = \Gamma(1-n) \times S_g(i\omega)^n. \quad (13)$$

The "gel strength"  $S_g$  depends on the mobility of the chain segments.  $\Gamma$  is the usual gamma function. The relaxation exponent of  $n$  adopts values between 0 and 1.  $i$  is the imaginary unit. The power function of frequency implies the property of mechanical selfsimilarity where  $G'(\omega)$  and  $G''(\omega)$  values are scaled with frequency.

The evolution of rheology can be observed continuously during the entire gelation process. For the state of the sample, the gelation process can be divided into three; those are pre-gel state, critical gel state and post-gel state. Then, it becomes understandable the evolution of rheology by taking the critical gel as the reference state. The three states are shown in Figure 4 schematically using the dynamic viscosity of  $\eta^*$  as the representative rheological property.

$$\eta^* = \frac{\sqrt{G'^2 + G''^2}}{\omega} \quad (14)$$

These three states are evidenced in the experimental data of polydimethylsiloxane. The progress of viscoelastic data with gelation can be accounted for using the plot of  $|\eta^*|$  and  $\omega$ . At high frequency, the power law behaviour of  $|\eta^*| \propto \omega^{-1}$  is exhibited. The sample appears to be at the gel point in this frequency window. However, at the pre-gel states, deviations from the power law dependence are seen as the frequency is lowered and the finite size of the largest cluster is recognisable. The low frequency behaviour is still that of a typical viscoelastic liquid which is described as,

$$G'(\omega) \propto \omega^2, G''(\omega) \propto \omega, \text{ in the limit } \omega \rightarrow 0. \quad (15)$$

Therefore the zero frequency viscosities,  $\eta_0$ , are determined for respective  $p$  values as shown in Figure 4. The characteristic frequency of  $\omega^*$  can be defined by the intersection of  $\eta_0$  with the power law of the critical gel.  $\omega^*$  divides between the gel and the liquid behaviours. The value of  $\omega^*$  decreases with approaching to the gel point.

In the post-gel region,  $p > p_c$  the polymer exhibits a finite equilibrium modulus of  $g_\infty$ . A characteristic frequency  $\underline{\omega}^*$ , can be defined again(see Figure 4) for respective  $p$  values. At high frequencies above some crossover  $\underline{\omega}^*$ , the sample shows the behaviour of critical gel state and at frequency below it, the sample behaves like a typical viscoelastic solid ( $G' = g_\infty$ ,  $G'' \propto \omega$  at  $\omega \rightarrow 0$ ).  $\underline{\omega}^*$  value increases with increasing the extent of cross-linking.

In the evolution of viscoelastic properties, the most interesting part of the rheological behaviour shifts to lower and lower frequencies as the transition becomes closer. The shift to



lower frequencies is so pronounced that the actual transition through the gel point cannot be observed in an experiment, because  $\omega^*$  has shifted below the lower limiting frequency of the rheometer. Only far beyond the gel point in the post-gel region, the characteristic frequency becomes large again, so the solid behaviour becomes measurable within the frequency range of the instrument.

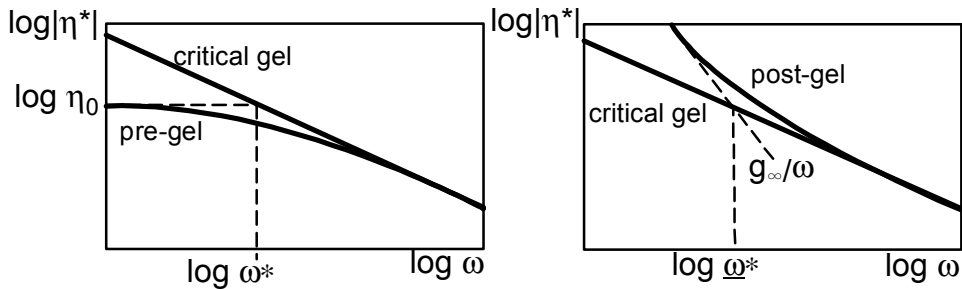


Fig. 4. Schematic representation for the relation of  $|\eta^*|$  vs  $\omega$  for three states of pre-gel, critical gel, post-gel, and the definition of the characteristic frequency,  $\omega^*$ ,  $\underline{\omega}^*$  of the pre-gel and the post-gel respectively.

Although the viscoelastic properties are sensitive to the frequency scales, the basic frequency-length relationship always can be applied, in the sense that high frequency probes smaller length scales, and low frequency probes large length scales. This is usually ruled by a dispersion relation between frequency, time and length.

$$\frac{1}{\omega} \propto t \propto L^\alpha \tag{16}$$

$t$  is relaxation time and  $L$  is the scale of observation.  $\alpha$  is an exponent, specific to the model considered. The mechanical selfsimilarity is the relation between viscoelasticity and frequency. Eq.(16) indicates the relation of frequency and  $L^{-\alpha}$ . From these fragments, the concept of selfsimilarity for network structure in critical gel are considered.(Cates, 1985; Muthukumar, 1985)

The power law behaviour of the critical gel correlates to a length scale range. Beyond the very wide frequency range, where power law appears at gel point, a lower frequency limit is expected to be given by the sample size and an upper frequency limit is given by the transition of single chain behaviour. If the frequency is large enough, length scales much smaller than self similar regions are probed, for example, finding the range of a single chain between two cross-links. Power law relaxation is observed when  $L$  has a value in the range between these lower and upper boundaries of lengths in the material.

The characteristic frequency  $\omega^*$  corresponds to a correlation length,

$$\omega^* \propto \xi^{-\alpha} \tag{17}$$

which is characteristic for the network structure. The structure is hypothesised to be selfsimilar at scales below  $\xi$ , as supported by mechanical selfsimilarity. Also a possible model has been given to support the hypothesis. The critical gel is treated as polymeric

fractal, that is, a selfsimilar object.  $\xi$  has to be identified by the size of the selfsimilar regions, i.e. the critical correlation length. We have seen the relation between  $\xi$  and  $p_c$  in Section 2.1.2, as  $\xi \propto |(p - p_c)/p_c|^{-\nu}$ , which implies  $\omega^* \rightarrow 0$  if  $p \rightarrow p_c$  and agrees with the above arguments.

The evolution of  $\xi$  with the progress of end-linking reaction is a direct expression of the evolution of network structure. In the pre-gel state, the molecules are taken into clusters by the end-linking reaction, which are weak solids of small spatial dimension. With the increase in reaction time, one gets larger and larger clusters. Assuming there are large clusters in the melt of smaller clusters and uncrosslinked chains, the mechanical experiment is sensitive to the size of a typical cluster. At longer reaction times this size becomes larger and larger until it extends across the entire sample. The size of the typical cluster becomes infinite at the gel point where the critical gel is formed. The network structure of the critical gel is self similar and so only a very large length matters. Generally one calls such self similar objects "fractals". The straight lines in  $G'(\omega)$ ,  $G''(\omega)$  over all  $\omega$  indicate that there is no dominant length scale in the polydimethylsiloxane sample, i. e. the correlation length is infinite and on each scale of observation a similar structure can be found.

## 2.2 Experimental approach for sol-gel transition

In the previous section, many power law dependences could be seen near gel point for various properties. In particular, the notion of mechanical selfsimilarity and structural selfsimilarity derived by the power law attracted many research workers. The experimental method that investigates dynamic viscoelasticity and frequency near gel point was adopted and many results have been reported for wide range of materials. Also the scaling concepts have been used frequently as an analysing method. The materials are; food, surfactant, liquid crystals, elastomer etc, which suggests that gelation is the universal phenomena and common to the compounds of large fields, and further the power law is applicable to the wide range. A part of examples are shown here; gelatin (Michon et al, 1993; Hsu & Jamieson, 1990), carrageenan (Hossain et al, 2001), ethyl(hydroxyethyl)cellulose and surfactant (Kjønixsen et al., 1998), soy protein (Caillard, et al., 2010), poly(vinyl alcohol) (Kjønixsen & Nyström, 1996), poly(urethane) network (Nicolai et al., 1997), liquid crystalline network (Valentva et al., 1999), pluronic triblock copolymer end-modified (Bromberg et al., 1999), poly(acrylonitrile) (Tan et al., 2009), asphalts (Vargas & Manero, 2011), hyperbranched poly( $\epsilon$ -caprolactone) (Kwak et al., 2005). The analytical approach which is common to these experimental examinations attempts, using a common scale, to estimate the gelation of different solvents, different chemical species, cross-links of different kinds. Among the research reports of conventional polymers, the experimental works for poly(vinyl chloride) (Li et al., 1997-1998) demonstrates obvious results on the relationships between viscoelasticity, concentration, temperature, molecular weight and so forth. The methods to determine scaling exponents experimentally are also shown for viscosities and elastic moduli. Those results are described in the following sections.

### 2.2.1 Concentration and gel strength

Aoki et al. prepared PVC gels from well-characterised poly(vinyl chloride) samples and the solvent of bis(2-ethylhexyl) phthalate (DOP). In the experiment, four PVC samples were used and the gelation of the solution was examined with PVC concentration as the variable

to dominate sol-gel transition. The weight-average molecular weight ( $M_w$ ) of the samples are  $39.4 \times 10^3$ ,  $87.4 \times 10^3$ ,  $102 \times 10^3$ ,  $173 \times 10^3$ , they are denoted as PVC4, 9, 10, 17, respectively.

$G'(\omega)$  and  $G''(\omega)$  data are shown in Figures 5 and 6 for the solutions of PVC4. The polymer concentration ranges from 9.8 to 154 g/L as indicated. At very low concentrations, the viscoelastic behaviour of PVC4 solutions follows that of a viscoelastic liquid as described by

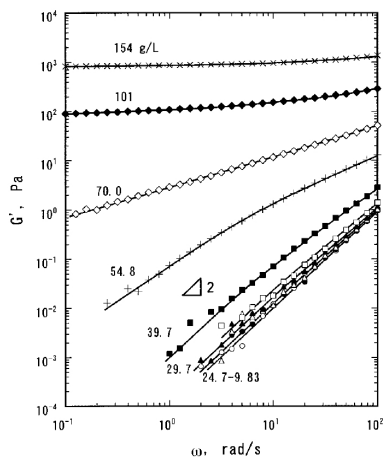


Fig. 5. Storage modulus  $G'$  of PVC/DOP as a function of  $\omega$  for various concentrations of PVC4 as indicated. Reproduced, with permission of the author.

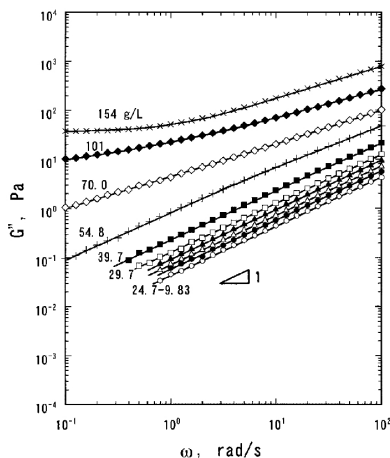


Fig. 6. Loss modulus  $G''$  of PVC/DOP as a function of  $\omega$  for various concentrations of PVC4 as indicated. Reproduced, with permission of the author.

eq.(15), while the deviation from the relation of eq.(15) becomes more pronounced with the increase in concentration. The result,  $G'(\omega)=\text{const.}$  at  $\omega \rightarrow 0$  indicates the formation of a gel plateau. The slope of the  $G'(\omega)$  vs  $\omega$  curve (at  $\omega \rightarrow 0$ ) in the double logarithmic plot changes

from 2 to 0, whereas that of the  $G''(\omega)$  vs  $\omega$  curve at  $(\omega \rightarrow 0)$  varies from 1 to 0. Furthermore, it is obvious at the gel point that both slopes take a common value between 0 and 1. The viscoelastic behaviour for other systems, PVC9, -10 and -17 was virtually same. The range of polymer concentration where the sol-gel transition is observed was dependent on the molecular weight of PVC.

Determination of gel point for PVC gel was conducted on the basis of the frequency-independence of  $\tan \delta$ , which is known as the method using a multifrequency plot of  $\tan \delta$  vs gelation time, temperature, or concentration, depending on which variable governs the gelation process. The gel point has been well determined using this method when the gelation time or temperature was a controlling variable for gelation. (Koike, 1996; Peyrelasse, 1996) Figure 7 shows the multifrequency plot of  $\tan \delta$  vs PVC concentration, where all curves pass through the single point at the certain PVC concentration, which can be defined as the gel point,  $c_g$ .

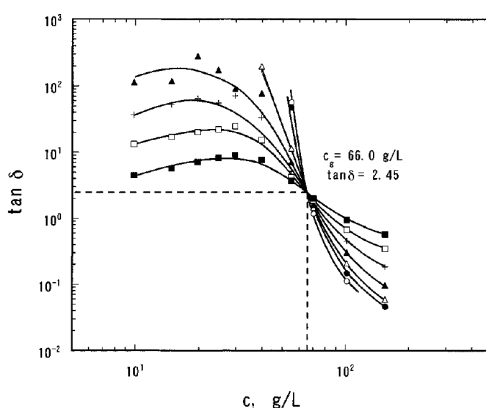


Fig. 7. plot of  $\tan \delta$  as a function of concentration of PVC4 for various frequencies. Reproduced, with permission of the author.

The well-used scaling law for the viscoelastic behaviour in the vicinity of the gel point is expressed in eq.(12) The equation of  $G(t)$ , the shear relaxation modulus, shown below is one of the deduced descriptions from eq.(12).

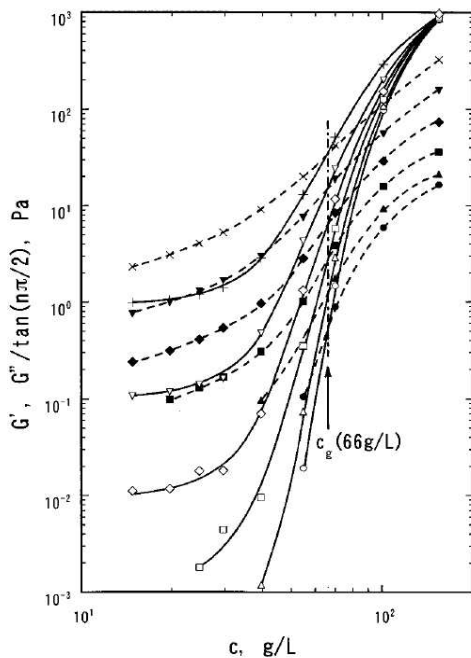
$$G(t) = S_g t^{-n} \quad (18)$$

$S_g$  is called as the gel strength and has an unusual unit of  $\text{Pa s}^n$ .  $n$  is named the critical relaxation exponent because  $n$  determines the stress relaxation rate at the gel point. One may simply understand that  $S_g$  is the relaxation modulus at the gel point when the relaxation time  $t$  equals 1s. The expression of  $S_g$  as  $S_g = G(t) \times t^n$  may be of help to understand the physical meaning of  $S_g$ .  $n=0$  gives  $S_g = G_0$ , the elastic modulus, that describes the rigidity of the sample. Also  $S_g$  represents the viscosity for  $n=1$ . A similar expression can be applied at the gel point for  $G'(\omega)$  and  $G''(\omega)$ .

$$G'(\omega) = \frac{G''(\omega)}{\tan(n\pi/2)} = S_g \omega^n \Gamma(1-n) \cos(n\pi/2) \quad (19)$$

The complex modulus seen in eq.(13) is rewritten to the storage and loss moduli in equation (19). Because the critical exponent  $n$  is determinable from  $\tan \delta$  value at the gel point shown in Figure 7,  $S_g$  can be calculated from  $G'(\omega)$  and  $G''(\omega)$  data at the gel point. (N.B.  $\delta=n\pi/2$ ).

Equation (19) suggests that there exists a crossover of  $G'(\omega)$  and  $G''(\omega)/\tan(n\pi/2)$  at the gel point.  $G'(\omega)$  value at the gel point is obtained by plotting  $G'(\omega)$  and  $G''(\omega)/\tan(n\pi/2)$  against PVC concentration, and then  $S_g$  would be easily calculated. Figure 8 is the plot of this kind for the PVC solutions. Since the solution at the gel point obeys the frequency independence of  $\tan \delta$ , all crossover points appear well at the gel point being consistent with Figure 7.



$\omega$ (rad/s)	0.316	1	3.16	10	31.6	100
$G'$ (Pa)	○	△	□	◇	▽	+
$G''/\tan(n\pi/2)$ (Pa)	●	▲	■	◆	▼	×

Fig. 8. Plots of  $G'$  and  $G''/\tan(n\delta/2)$  against polymer concentration  $c$  for the PVC4 system.  $\omega$ , the frequency was varied from 0.316 to 100 rad/s.  $n=0.75$  was used to calculate  $G''/\tan(n\delta/2)$ .  $c_g$ , gel point is indicated by the arrow. Reproduced, with permission of the author.

### 2.2.2 Divergence of viscosity

In the previous section, detail of the frequency power law was described for PVC solution as an example of experimental gelation system. Moreover, rheological studies are seen in this section by focusing on how the zero shear viscosity,  $\eta_0$ , diverges when the gelling system goes close to the gel point from the solution of low concentration.

Concerning the divergence of  $\eta_0$ , the scaling law of eq.(10) has already mentioned as a critical behaviour near the gel point. Equation (10) was issued for  $p < p_c$ , and  $p$  can be, for example, the extent of reaction for crosslinking, gelation time, temperature;  $k$  is the critical exponent determining the critical characteristics near the gel point. Experimental determination for  $k$  is not difficult provided that  $p_c$  is known. If  $p_c$  is unknown, eq.(20) is useful for the simultaneous determination of  $p_c$  and  $k$ .

$$\frac{-\eta_0^{-1}}{d\eta_0^{-1}/dp} = \frac{p_c - p}{k} \quad (20)$$

Equation (20) is given by transforming eq.(10), then the values of  $p_c$  and  $k$  are acquired from the slope and intercept of the plot of  $-\eta_0^{-1}/(d\eta_0^{-1}/dp)$  vs  $p$ . Aoki et al. demonstrated that this plot works efficiently to determine  $p_c$  and  $k$  from the data of  $G'(\omega)$  and  $G''(\omega)$  of PVC solution.(Li, 1997a)

In their work, three samples of PVC4, PVC9, PVC17 were used for dynamic viscoelasticity measurements of pre-gel samples. Figure 9 shows the plot of  $\eta^*$  vs  $\omega$  for PVC4 solutions of various concentrations.  $\eta^*$  is derived using eq.(14). Solutions of  $c$  lower than 59.9g/L show  $\eta^*$  of the frequency-independence at  $\omega \rightarrow 0$ , which enable to determine  $\eta_0$ . The range of frequency-independence shifts to lower frequency side as the increase in  $c$ . Eventually, the frequency-independent behaviour shifts below the lower limiting of the rheometer, which has already mentioned in Figure 4. Note that  $c_g$  of PVC4 solution is 66g/L. In fact, PVC4 of  $c=62.9\text{g/L}$ , slightly lower than  $c_g$ , does not show the frequency independence. Also for solutions of other PVC systems of the concentrations slightly lower than  $c_g$ , similar behaviour is observed.

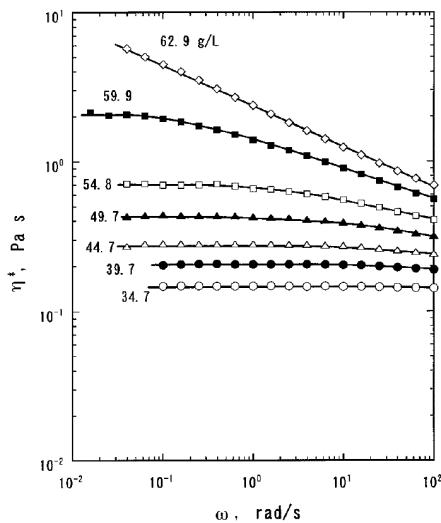


Fig. 9. Complex viscosity  $\eta^*$  as a function of  $\omega$  for PVC4/DOP samples. The PVC concentration ranges from 34.7 to 62.9g/L as indicated. Reproduced, with permission of the author.

Before constructing the plot of eq.(20),  $\eta_0^{-1}$  was plotted against  $c$  as shown in Figure 10 to calculate  $d\eta_0^{-1}/dc$ . N.B.  $p$  corresponds to  $c$  in this experiment. Then  $-\eta_0^{-1}(d\eta_0^{-1}/dc)^{-1}$  was calculated. Figure 11 shows that linear relations are obtained for  $-\eta_0^{-1}(d\eta_0^{-1}/dc)^{-1}$  and  $c$  for PVC4, PVC9, PVC17 solutions. The slope of the straight line is equivalent with  $-1/k$ , the intercept of x-axis is equivalent with  $c_g$ . As compared to  $c_g$  value obtained by the method of frequency independence of loss tangent(see Fig. 7),  $c_g$  value of the method of Fig. 11 varied within a deviation of about  $\pm 7\%$ . The variation for  $k$  values of these two methods were also within about  $\pm 7\%$ , one is obtained from the plot of  $\eta_0$  vs  $(c_g - c)/c_g$  in double logarithmic scale with  $c_g$  of Fig. 7 method, the other one is from Fig. 11 method.

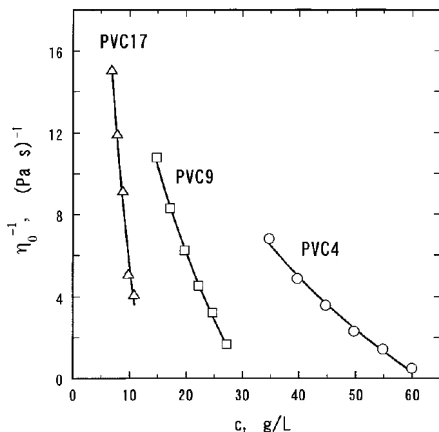


Fig. 10.  $\eta_0^{-1}$  plotted as a function of PVC concentration,  $c$ , for PVC4, PVC9 and PVC17 solutions. The solid lines are obtained by fitting to the linear function of  $\log c$ .

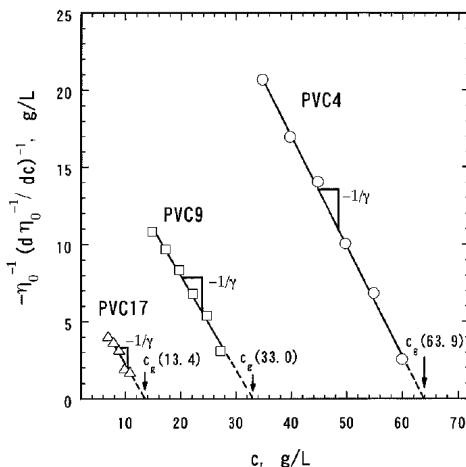


Fig. 11. Plots of  $-\eta_0^{-1}(d\eta_0^{-1}/dc)^{-1}$  vs polymer concentration  $c$  for PVC4, PVC9, and PVC17 systems. For each gelling system, a linear fitting of the data gives simultaneously the value of exponent  $k$  and the critical concentration  $c_g$ .

The advantage of Fig. 11 method is the simultaneous determination of  $c_g$  and  $k$ . However, there is also disadvantage in Fig. 11 method, that is, the error level is high in the determination of  $d\eta_0^{-1}/dc$  from Figure 10 in which the ranges of  $\eta_0^{-1}/dc$  and  $c$  are not wide enough.

### 3. Delay of gel point and ring formation

In relation to properties of gels, many research works have been carried out to predict gel point for the gelation of  $RA_{f_a} + R'B_{f_b}$  type polymerisation.  $RA_{f_a}$  and  $R'B_{f_b}$  are monomers with functionalities of  $f_a$  and  $f_b$  respectively. Although the system appears to be limited to the network formed by polymerising monomer, it can be generalised by selecting  $f_a$  and  $f_b$  appropriately or modifying the reactive species. Flory presented the most simple description of gel point as shown in eq.(21), often called as the classical theory.(Flory, 1941)

$$(f_a - 1)(f_b - 1) \times p_a p_b = 1 \quad (21)$$

A more simple expression has already described in eq.(1).  $p_a$  and  $p_b$  are the extent of reaction for reactive groups A and B, respectively. In deriving eq.(21), some ideal reactions are considered, in which following two assumptions are used; all like groups have equal reactivities, and there is no intramolecular reaction. Conversely, if unequal reactivity and the intramolecular reaction are included in the polymerisation, the extent of reaction at gel point shifts to higher value than that of eq.(21), and beyond the gel point the equilibrium modulus is lowered. The intramolecular reactions cause ring structures in network which are elastically inactive chains. Accordingly, it is possible to estimate the amount of intramolecular reaction and to quantify the unequal reactivity by establishing suitable model and measuring the gel point shift experimentally.

Recently, Tanaka et. al developed the gelation model for the polymerisation of epoxy and diamine including the effects of unequal reactivity and intramolecular reaction, where the ring-forming parameter was introduced to characterise the competition between intermolecular and intramolecular reactions.(Tanaka, et al., 2009) This section is concerned with the gelation model developed and its application to the polymerisation of polyoxypropylene (POP) diamine and the diglycidyl ether of bisphenol A (DGEBA),  $RA_4 + R'B_2$  type polymerisation.

#### 3.1 Gel point in the network formation by $RA_4 + R'B_2$ type polymerisation

A reaction scheme was defined for a POP diamine with four reactive hydrogen atoms, and DGEBA having two epoxy groups. There are two features required for defining the scheme; to follow the progress of the reaction by the extent of reaction,  $p$ , and to incorporate the ring-forming parameter as shown later.

In the course of network formation, the primary amine in POP diamine and an epoxy group in DGEBA react with a rate constant  $k_1$ , then the secondary amine formed and an epoxy group react with a rate constant  $k_2$  to form the tertiary amine. Hydrogen atoms are categorised as being in states H1, H2 and HR according to the reactions. That is, the hydrogen atoms that belong to unreacted amino groups are defined as H1, the unreacted hydrogen atoms that belong to the semireacted amino groups are defined as H2, and reacted hydrogen atoms are defined as HR. In the reaction of rate constant  $k_1$ , two H1 atoms are lost,



and one H2 atom and one HR atom are formed. In the reaction of  $k_2$ , one H2 atom is lost and one HR atom is formed.

The concentrations of H1, H2, HR atoms and epoxy groups, are written as  $c_{H1}$ ,  $c_{H2}$ ,  $c_{HR}$  and  $c_{EP}$  respectively. Let the concentration of H1 and epoxy groups before the reaction (i.e.  $t=0$ ) be  $c_{H1}^0$ ,  $c_{EP}^0$ , then  $p_{HR}$ , the extent of reaction of hydrogen atoms is,

$$p_{HR} = c_{HR} / c_{H1}^0 \tag{22}$$

$p_{HR}$  is the variable to dominate the gelation, and is directly measurable by FT-IR spectroscopy for the reaction of POP diamine and DGEBA. (Mijovic, 1995) Furthermore,  $p_{HR}$  can easily be incorporated into the equation of chain growth expressed in terms of the probability of paths shown below.

The rates of change of the concentrations of H1, H2 and HR are given by the following equations;

$$dc_{H1}/dt = - 2 k_1 \times c_{H1} \times c_{EP} \tag{23}$$

$$dc_{H2}/dt = k_1 \times c_{H1} \times c_{EP} - k_2 \times c_{H2} \times c_{EP} \tag{24}$$

$$dc_{HR}/dt = k_1 \times c_{H1} \times c_{EP} + k_2 \times c_{H2} \times c_{EP} \tag{25}$$

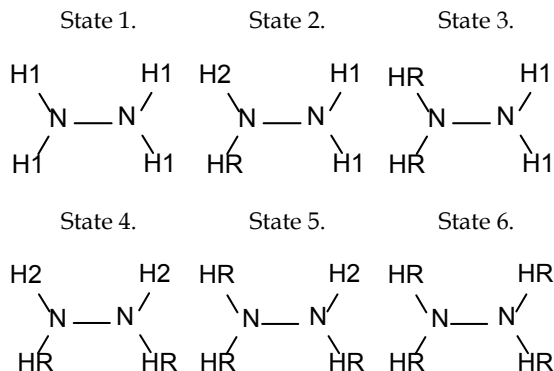


Fig. 12. Classification of the state of reaction for POP diamine unit in the progress of polymerisation. Numbers are placed as State  $i$ ,  $i=1-6$ .

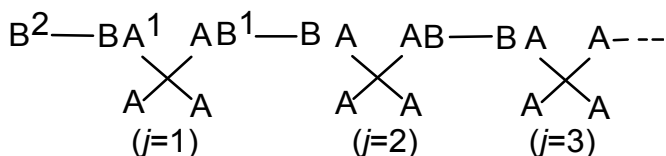


Fig. 13. Linear sequence of reactive units used to show chain growth and to define the size of the ring structure,  $j$ . The reactive group A corresponds to H atom of the amino group and the group B to epoxy group.

The progress of the reaction can be monitored by solving the rate equations of eqs.(23-25) with experimental conditions. That is, the relations of  $p_{H1}$  vs  $p_{HR}$  and  $p_{H2}$  vs  $p_{HR}$  are obtained with the parameter of  $\rho$  ( $=k_2/k_1$ ), the rate constant ratio, where  $p_{H1}=(c_{H1}/c^0_{H1})$ ,  $p_{H2}=(c_{H2}/c^0_{H1})$ ,  $p_{EP}=(c_{EP}/c^0_{EP})$ .  $p_{H1}$  decreases monotonously, while  $p_{H2}$  increases in the first half then decreases during the progress of polymerisation to completion.  $\rho$  is the index of the unequal reactivity;  $\rho=1$  if H1 and H2 are in equal reactivity, the increase in  $\rho$  more than 1 means the reactivity of H2 is higher than that of H1.

Six states of the diamine unit can be defined as shown schematically in Figure 12. The classification of the diamine unit shown here is similar to that of Dušek et al.(Dušek, 1975). However, its use to define the gel point is different. The gel point in the study of Dušek et al. is defined as the point of divergence of the weight- average molar mass. Whereas the gel point is derived in terms of the probabilities of continuing of paths in this work so as to incorporate experimentally measurable value of  $p_{HR}$  into them.

If the mole fractions of the six states are written as  $X_i$ ,  $i=1-6$ , they can be expressed as functions of  $p_{H1}$ ,  $p_{H2}$  and  $p_{HR}$ . Hence, the  $X_i$  are functions of  $p_{HR}$ .

	State 2		State 3		State 4		State 5		State 6
H atom	H1, H2	HR	H1	HR	H2	HR	H2	HR	HR
Probability*	$\frac{3}{4}$	$\frac{1}{4}$	$\frac{1}{2}$	$\frac{1}{2}$	$\frac{1}{2}$	$\frac{1}{2}$	$\frac{1}{4}$	$\frac{3}{4}$	1
Number of paths	1	0	2	1	2	1	3	2	3

\* Probability to chose the specified H atom.

Table 2. Probability of choosing and number of paths for each H atom of amino group in the chain growth.

To define the gel point, the probability of path continuation is introduced. The assumed linear sequence of structural units used to define gelation in the reaction of DGEBA and POP diamine is shown in Figure 13, which follows ARS theory.(Ahmad, 1980) The reactive group A corresponds to an H atom of the amino group and the group B to an epoxy group. The variable  $j$  gives the size of the ring. Suppose that the chain in Figure 13 grows from right to left, then  $\gamma_a$  is defined as the probability of a continuing path from a diamine unit attached to a randomly chosen H atom to the next diamine unit. Likewise,  $\gamma_b$  is defined as that of a continuing path from DGEBA unit attached to a randomly chosen epoxy group to the next DGEBA unit.

In order to obtain the expression of network formation, we need to consider the probability of continuing paths from a randomly chosen group to a statistically equivalent group; for example, a path from B<sup>1</sup> to B<sup>2</sup> in Figure 13. Let the fractions of A and B groups be  $X_a$  and  $X_b$  respectively, then the probability of continuing path,  $\gamma$  can be given as below;

$$\gamma = X_a\gamma_a + X_b\gamma_b . \quad (26)$$

In order to derive the expression of  $\gamma_a$ , the probability of chain growth from a diamine unit to next diepoxy unit is considered in terms of the states of diamine unit and the count of the

number of continuing paths. If a diamine unit of State 2 is chosen, more specifically, an HR atom in State 2 is chosen, then it gives no paths out. If it is either an H1 or H2 atom, it gives one path out, which is HR in State 2. Because the probability that either an H1 or H2 atom is chosen in State 2 is  $3/4$  (see Figure 12), the contribution from State 2 to the chain growth is  $3X_2/4$ ; it is given by the product of the number of paths and the probability. The probabilities that individual H atom is chosen and the number of paths out in each state of POP diamine unit are summarised in Table 2. The probability of chain growth from diepoxy to next diamine unit is  $p_{EP}$ . Hence,  $\gamma_a$  can be expressed by  $p_{EP}$  and the total of the contributions from the respective state of diamine unit.

$$\gamma_a = \left( \frac{3}{4} X_2 + \frac{3}{2} X_3 + \frac{3}{2} X_4 + \frac{9}{4} X_5 + 3X_6 \right) \times p_{EP} \quad (27)$$

Similarly,  $\gamma_b$  can be expressed using  $X_i$ ,  $i=1-6$  and  $p_{EP}$ .

The calculation results of  $\gamma$  as a functions of  $p_{HR}$  are shown in Figure 14.  $\rho$  values used for the calculations are 1, 0.5, 0.1. The  $\gamma$  value increases from 0 to 3 as  $p_{HR}$  increases from 0 to 1. The result that  $\gamma=3$  as  $p_{HR}=1$  comes from the fact that functionalities of POP diamine and DGEBA are 4 and 2 respectively; when all the groups are reacted POP diamine units are all in State 6 which has 3 paths of continuation from a randomly chosen reacted amino group.

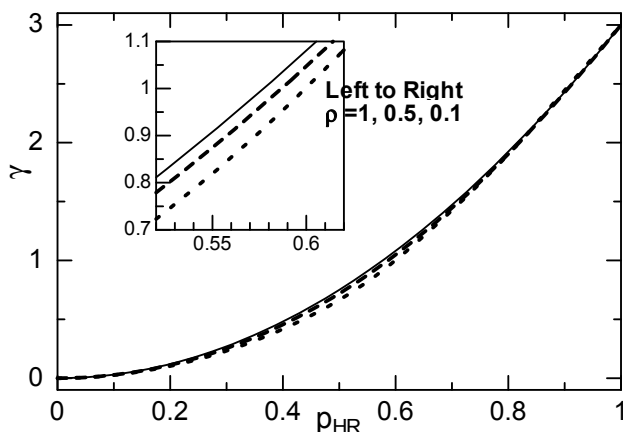


Fig. 14. The results of calculation for  $\gamma$  as functions of  $p_{HR}$  with different  $\rho$  values; solid thin line:  $\rho=1$ , dashed line:  $\rho=0.5$ , dotted line:  $\rho=0.1$ . The inset figure magnifies near  $\gamma=1$ .

Curves of  $\gamma$  vs  $p_{HR}$  depend on  $\rho$ , as can be seen in the inset figure, which is the effect of unequal reactivity on the path continuation.  $p_c$ , the value of  $p_{HR}$  at  $\gamma=1$  is  $p_c=0.577$  for  $\rho=1$  which agrees with the value calculated from eq.(21). Note that we have  $p_a=p_b$  as the experimental condition. As  $\rho$  decreases  $p_c$  shifts to a higher value, which is confirmed to come from the dependence of the  $\gamma_b$  vs.  $p_{HR}$  curve on  $\rho$ . The shift of  $p_c$  is the delay of gel point. The decrease in  $\rho$  means less reactions of  $k_2$ ; that is, formation of State 3, 5 and 6 is delayed. State 5 and 6 brings about bifurcation that leads to the gelation. In other words, the delay of gel point with the decrease in  $\rho$  is caused by the delay of formation of State 5 and 6.

### 3.2 Ring-forming parameter

For an  $RA_4+R'B_2$  type polymerisation, competition always occurs between intermolecular and intramolecular reaction. In the competition between intermolecular and intramolecular reaction, let  $c_{b,int}$  be the internal concentration of B groups from the same molecule around an A group being on the point of reacting, and let  $c_{b,ext}$  be the concentration of B groups from other molecules. Then, the ring-forming parameter  $\lambda_b$  can be given concerning B group as;

$$\lambda_b = c_{b,int} / (c_{b,ext} + c_{b,int}), \quad (28)$$

$c_{a,int}$  and  $c_{a,ext}$  can be similarly defined when a B group is about to react with an A group. The definition of  $\lambda_a$  is as follows.

$$\lambda_a = c_{a,int} / (c_{a,ext} + c_{a,int}) \quad (29)$$

The size of the ring structure can be given by  $j$  as shown in Figure 13. For example, the smallest ring structure is comprised of a pair of POP diamine and DGEBA units. This structure is regarded as that of  $j=1$ . The second smallest ring consists of two of each unit and is regarded as the structure of  $j=2$ . In consequence,  $c_{b,int}$  is the total of the concentration of each size.

$$c_{b,int} = \sum_{j=1}^{\infty} c_{b,int,j} \quad (30)$$

$c_{b,int,j}$ ,  $j=1, 2, \dots$  is the concentration of the B groups to form each size of the ring structure around an A group. Likewise,  $c_{a,int}$  can be written by the total of the concentration of the A groups to form each size of the ring structure around the B group.

$$c_{a,int} = \sum_{j=1}^{\infty} c_{a,int,j} \quad (31)$$

In counting the concentration  $c_{b,int,j}$ , it is necessary to consider a specific feature of the ring structure; that is, it can be thought of as a chain which end-to-end distance is equal to zero. It is assumed that the distribution of end-to-end distance can be written by independent Gaussian sub-chain statistics of eq.(32) for the polymer chain including POP diamine and DGEBA.

$$P(r) = \left(\frac{3}{2\pi\nu b^2}\right)^{3/2} \exp\left(-\frac{3r^2}{2\nu b^2}\right) \quad (32)$$

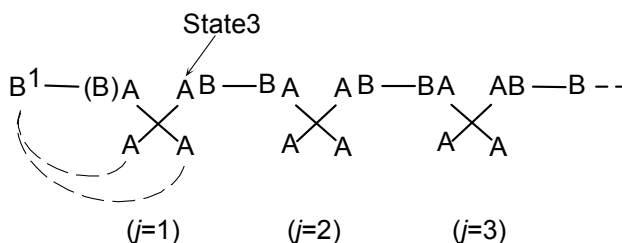


Fig. 15. Occurrence of an unreacted B group,  $B^1$ , on  $RA_4$  unit in State 3, giving the possibility of A group reacting intramolecularly to form a ring structure of the smallest size.

$$\langle r^2 \rangle = \nu b^2 \quad (33)$$

$r$  is end-to-end vector.  $b$  is the effective bond length of the chain of  $\nu$  bonds. In particular, if a definition is given on  $P_{ab}$  with substituting  $r=0$  and dividing by  $N_{av}$ , Avogadro's number, then it becomes a useful parameter in counting the concentration of  $c_{a,int,j}$  and  $c_{b,int,j}$ .

$$P_{ab} = \frac{1}{N_{AV}} \left( \frac{3}{2\pi \langle r^2 \rangle} \right)^{3/2} \quad (34)$$

Similar approach to describe intramolecular reaction has been reported for  $RA_3 + R'B_2$  type polymerisation. (Jacobson & Stockmayer, 1950)  $P_{ab}$  means the concentration of intramolecular B groups of  $j=1$  around an A group; it can also be said that it means the concentration of intramolecular A groups of  $j=1$  around a B group.

Consequently, eq.(30) can be calculated as follows;

$$c_{b,int} = \sum_{j=1}^{\infty} \frac{1}{N_{AV}} \left( \frac{3}{2\pi \langle r^2 \rangle} \right)^{3/2} = P_{ab} \sum_{j=1}^{\infty} \left( \frac{1}{j} \right)^{3/2} = 2.61 P_{ab}. \quad (35)$$

In the above calculation Truesdell function was taken into account. (Truesdell, 1945) Similarly,  $c_{a,int} = 2.61 P_{ab}$  can be given and an expression of  $\lambda_a$  is derived;

$$\lambda_a = P_{ab} / c_a^0 \quad (36)$$

where  $c_a^0$  is the concentration of A group before the reaction and  $c_a^0 = c_{HI}^0$  in this work.

### 3.3 The gel point expression including ring formation

In order to obtain an expression for  $\gamma$  into which the ring-forming parameter was incorporated, path continuations both from diamine to diamine units and from diepoxy to diepoxy units, and the intramolecular reactions are considered simultaneously. Suppose that the randomly chosen group is H atom in the amino group, i.e. A group. Then, the contribution to the probability of continuing path,  $\gamma_a$ , is considered taking account of the internal concentration according to the states of diamine unit. Hence, we have  $\lambda_{ai}$  with  $c_{a,int,i}$ ,  $i=2-6$ .

$$\lambda_{ai} = c_{a,int,i} / (c_{a,ext} + c_{a,int,i}) \quad (37)$$

For example,  $c_{a,int,2}$  is the concentration of intramolecular A group when a B group continuing from POP diamine unit in State 2 is about to react. If there is no ring formation, the diamine unit of State 2 contributes  $(3/4)X_2 \times p_{EP}$  to the path continuation. The formation of the ring reduces the contribution by a factor of  $\lambda_{a2}$ ; that is, the contribution of the diamine unit of State 2 to  $\gamma_a$  can be expressed as  $(3/4)X_2 \times p_{EP}(1-\lambda_{a2})$ .

From the similar arguments for  $\lambda_{ai}$ ,  $i=3-6$  as well as  $\lambda_{bi}$ , the equations corresponding to eq.(27), and hence eq.(26) can be given to be solved under  $\gamma=1$ . Figure 15 illustrates the possible intramolecular reaction to form a ring structure of the smallest size when a randomly chosen unreacted A group is on an  $RA_4$  unit in State 3 to calculate  $c_{a,int,3}$ .

As a consequence of the network model, the relation between  $p_c$  and  $P_{ab}/c_{HI}^0 (= \lambda_a)$  is obtained (see Figure 16.) which tells the internal concentration of the reactive group A shown by eq.(25)

at the moment that the solution of POP diamine and DGEBA comes to gel point of  $p_c$ . For  $\rho=1$ , Figure 16 shows  $p_c=0.577$  at  $P_{ab}/c_{HI}^0=0$ , which corresponds with the gel point of eq.(21).  $p_c$  increases with  $(P_{ab}/c_{HI}^0)$ , which implies that the more intramolecular reactions cause the delay of gel point, as  $P_{ab}$  determines how likely the growing polymer chain forms a ring structure.

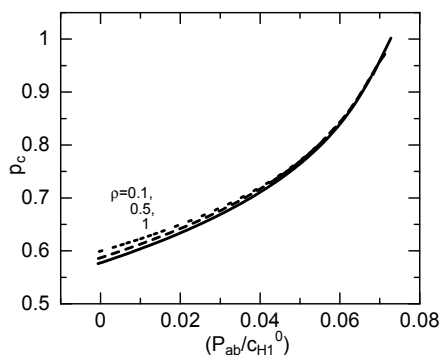


Fig. 16. The relation between  $p_c$  and  $(P_{ab}/c_{HI}^0)$  calculated for different  $\rho$  values.  $\rho=0.1, 0.5, 1$  are used.

$p_c$  of Figure 16 can be applied to the gel points of experimentally measured values to find the ring-forming parameter of  $\lambda_a$ ; note that  $c_{HI}^0$  is also an experimental value evaluated from the concentration of POP diamine in the solution. Figure 17 shows the results for POP diamine of various chain lengths; the plots lie on straight lines through the origin which corresponds with the gel point expressed by eq.(21). From the slope of the plot  $P_{ab}$  is determined. Because  $P_{ab}$  is a function of  $\langle r^2 \rangle$ , the chemical structure of monomer reactants determine the value of  $P_{ab}$ .

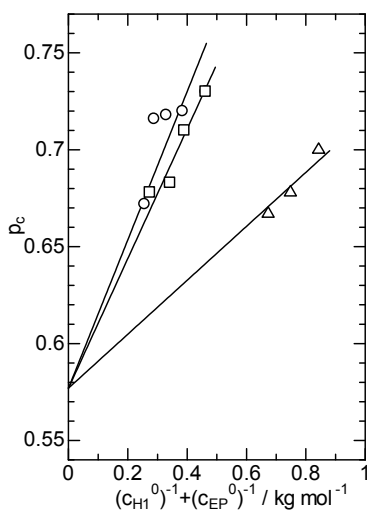


Fig. 17.  $p_c$  plotted against  $(c_{HI}^0)^{-1} + (c_{EP}^0)^{-1}$  for polymerisation systems of various POP diamines Nominal molecular weight for the POP chain:  $M_n=230$ (Circle),  $400$ (Square),  $2000$ (Triangle).

#### 4. Network formation by end-linking of star polymer

For entangled linear flexible polymers, the viscoelastic relaxation in response to mechanical deformation is the long-standing problem and has been extensively studied. (Ferry, 1970) The response is solid-like at high frequencies for a given temperature, but often some relaxation occurs due to localised motion. At lower frequencies the system relaxes due to cooperative motion of the segments in the chain backbone. The lower the frequency is, the larger the size of the chain backbone that can relax its conformation in response to the deformation. The situation written above is of more interest for polymers having bifurcation. Furthermore, the extension of the idea to the connection of polymers having bifurcation is also possible.

The end-linking of star polymers is an example of the connection of polymers having bifurcation, and generates a branched polymer of complex architecture. Increasing the connectivity extent ( $p$ ) leads to the formation of larger branched polymers until at a critical value ( $p_c$ ) a gel is formed. Viscoelastic behaviour of the star polymer is also of importance in terms of polymer chain dynamics of the melt and concentrated solution. Some recent experimental studies clarifies the molecular origins of the position of plateau and terminal flow for star polymers having arm chains which molecular weight is higher than the entanglement molecular weight.

As for the end-linking, an experimental work has already been published for the viscoelastic relaxation of poly(propylene sulfide) star by Nicol et al., they discussed the relation of  $p$  and viscoelasticity in detail. (Nicol et al, 2001) It is a 3-arm star polymer and can be end-linked by the reaction with hexamethyl diisocyanate (HMDI) in the presence of a small amount of catalyst of dibutyl tin dilaurate. Also, it is regarded as a network formation of  $RA_3 + R'B_2$  type reaction. (The values are functionalities.) The characteristic features to remark for poly(propylene sulfide) star, abbreviated as PPS star, is low  $T_g$  ( $\approx -37^\circ\text{C}$ ).

In relation to the experimental studies of the star polymer, an advanced calculation method for the viscoelasticity has been presented recently. The method based on the theory of tube model can be applied to the polymers of complex architecture. It is called as Branch-On-Branch Rheology (BOB) and has an advantage where branched polymers of different species can be mixed. (Das, 2006a; Das, 2006b) In addition, the polymer generate routine was incorporated in BOB to produce branched polymer by end-linking star polymers, which makes it possible to calculate  $G'(\omega)$  and  $G''(\omega)$  data for polymers of complex architecture. (Tanaka, 2008) This section is concerned with the comparison of  $G'(\omega)$  and  $G''(\omega)$  data between those calculated and experimental values which were supplied by the author of the original article. The data shown here are for the end-linked polymers with  $p$  lower than  $p_c$ , the gel point of connectivity. That is, those are viscoelastic behaviour of pre-gel state.

##### 4.1 Poly(propylene) sulfide star and end-linking

Three samples of PPS star are taken as the objects of BOB calculation. The code names are T5, T6, T7. The weight-average molecular weights ( $M_w$ , in the nominal unit of kg/mol) of PPS star are 18.9, 35.5, and 71.2 for T5, T6, and T7 respectively. Numbers of repeating unit in the arm,  $n_a$ , are 72, 128, 263 for T5, T6, T7. The entanglement molecular weight,  $M_e$  of PPS is 4000. In the preparation of PPS star, it is inevitable that the dimer of the star polymer is

produced by the coupling reaction of two -SH groups located at the chain ends. The coupling ratio ratios are 13, 12, 17% for T5, T6, T7.

Concerning the end-linking reaction, hydrogen atoms of -SH groups in the chain ends can be classified as H(1), H(2), H(3) and H(R), as shown in Figure 18. The classification enables us to describe the progress of reaction and the variation of the state of reaction of PPS star. Four states can be realised for PPS star according to the reaction; the mole fraction of each state was defined as  $x_i$ ,  $i=1, 2, 3, 4$ . In the macromolecule generated through the reaction, PPS star of the respective state will be allocated as follows; State 2 is in the end of the macromolecules, State 3 is in the backbone, State 4 is in the branching.

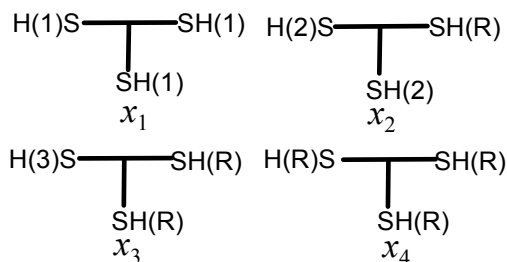


Fig. 18. Schematic representation for the state of reaction of PPS star unit. Reactive hydrogen atoms were classified as H(1), H(2), H(3) and H(R).  $x_1-x_4$  are fractions of the respective state of PPS star unit.

As for the hydrogen atom, H(1) is an unreacted atom, H(R) is the reacted atom. H(2) and H(3) are also unreacted hydrogen atoms but included in PPS star having one and two H(R) respectively. The value of  $p$  can be given as follows with the concentration of the hydrogen atoms,  $c_{H1}$ ,  $c_{H2}$ ,  $c_{H3}$ ,  $c_{HR}$ .

$$p = c_{HR} / (c_{H1} + c_{H2} + c_{H3} + c_{HR}) \quad (37)$$

The relationships between the number of the hydrogen atoms and the state of reaction can be written as; three H(1) are in State 1, two H(R) are in State 2 and one H(3) is in State 3. Also, H(R) are one in State 2, two in State 3 and three in State 4. As a practical meaning,  $p$  is equivalent with the experimentally determinable value of the connectivity extent. Further, rate equations were constructed for reactions from State 1 to State 2, from State 2 to State 3, from State 3 to State 4 with giving rate constants of  $k_1$ ,  $k_2$ ,  $k_3$  for respective reaction.

By solving the rate equations, the relation of  $x_1$  and  $p$  was obtained with choosing suitable value for the ratio of rate constants,  $\rho_0$  and  $\rho_1$ , as a fitting parameter.

$$\rho_0 = k_2/k_1, \rho_1 = k_3/k_2 \quad (38)$$

Figure 19 shows the result Of calculation for the relation of  $x_1$  and  $p$  for PPS star unit of State 1. The experimental value of  $x_1$  was also displayed in the figure; note that  $x_1$  is the fraction of PPS star monomer and can be estimated with SEC experiment. It clearly shows that  $\rho_0=0.667$  and  $\rho_1=0.5$  reproduced well the experimental result of  $x_1$ . These values correspond with the ratio of the number of unreacted -SH group, which implies the reaction between -SH group



and isocyanate group took place in proportional to the number of unreacted -SH group. Namely, the effect of induced unequal reactivity is negligible for the end-linking of PPS star. In the calculation of viscoelasticity shown below, the effect of unequal reactivity was not taken into account.

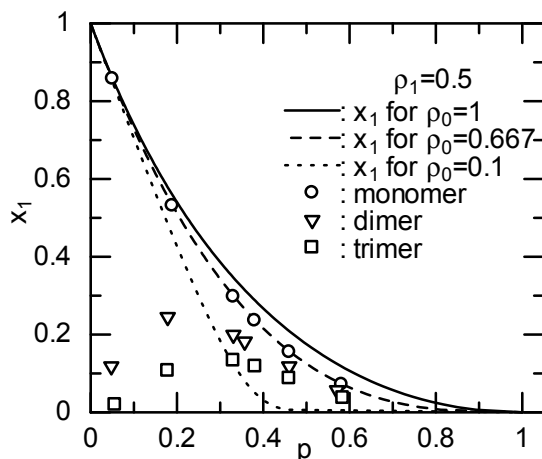


Fig. 19. Results of calculation on the mole fraction for PPS star unit of State 1 defined in Figure 18. Data obtained with  $\rho_1=0.5$ ,  $\rho_0=0.1, 0.667$  and 1 are displayed. The weight fractions of the first three oligomers in the end-link reaction determined by SEC measurement were added for comparison.

#### 4.2 Evolution of viscoelasticity by end-linking

The experimental results were shown in Figure 20(a), (b), (c) as the master curves of  $G'(\omega)$  and  $G''(\omega)$  for PPS star of T5, T6, T7 before end-linking, respectively. From DSC measurement, glass transition temperature ( $T_g$ ) of PPS star was determined around 236K. The maximum peaks for  $G''(\omega)$  which correspond with  $T_g$  appear in the master curves of higher frequency regions for T6 and T7. As lowering the frequency, both  $G'(\omega)$  and  $G''(\omega)$  gradually decrease and come to the plateaus.

The plateau modulus,  $G_0$ , was calculated using the equation written below, then viscoelasticity curve was calculated by BOB rheology for three arms star polymer, which results were also shown in Figure 20.

$$G_0 = \frac{4}{5} \frac{dRT}{M_e} \quad (39)$$

$d$  is density of PPS star,  $R$  is gas constant,  $M_e$  the entanglement molecular weight.

The effect of coupling reaction was considered in the viscoelasticity calculation of three arms star polymer. As mentioned above, the preparation of the star polymer accompanies the coupling reaction which mainly generates the dimer. It is obvious that the dimer is in the architecture of H-polymer, therefore the calculations were carried out with mixing three

arms star and H-polymer. The mixing ratio was chosen with reference to the coupling ratio of PPS star. As for the specification of H-polymer, the molecular weights of the side arm and cross bar,  $M_{\text{arm}}$  and  $M_{\text{bar}}$  respectively, were taken as follows;

$$M_{\text{arm}} = M_{\text{unit}} \times n_a, M_{\text{bar}} = M_{\text{unit}} \times 2n_a \quad (40)$$

where  $M_{\text{unit}}$  is the molecular weight of the repeating unit.

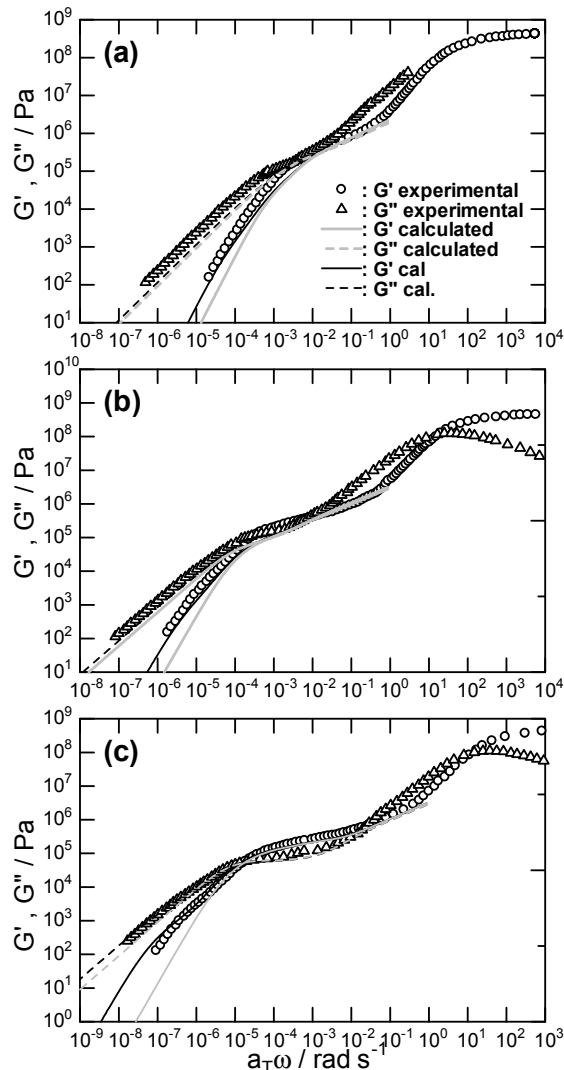


Fig. 20.  $G'$  and  $G''$  for different PPS stars before end-linking. (a) T5, (b) T6, (c) T7. Plots are measured data, curves are calculation data. Thicker lines are for PPS stars alone, thinner lines are for PPS stars mixed with H-polymer.

As a result of BOB calculation before mixing H-polymer (the grey thicker lines in Figure 20 which are denoted as PPS stars alone), the experimental and calculation data agreed well around the plateaus for T5, T6, T7. However, the difference between the experiment and calculation became distinguishable as the increase in  $n_a$  in the frequency range lower than the plateau.

Contrary to the data of PPS star alone, for those of H-polymer mixing (the black thinner lines), the terminal flows shifted to lower frequency sides in comparison with those of PPS star alone; the shift increased with the increase in  $n_a$ . It is concluded that the reproducibility between the experimental and calculation data was improved by the mixture of H-polymer.

The experimental result of T7 after end-linking was shown in Figure 21 for the sample having the connectivity extent of 0.41. The calculation data of  $p=0.41$  were added to the figure. The master curve of the experimental data was obtained for the reference temperature of  $T_{ref}=237K$  and for the frequency range ( $a_T\omega$ ) of  $10^{-11} \leq a_T\omega \leq 10^{-2}$  rad  $s^{-1}$ . Any clear plateau region was not shown for  $G'(\omega)$ . As for  $G''(\omega)$ , two ambiguous plateau regions appeared around  $a_T\omega = 10^{-4}$  and  $10^{-8}$  rad  $s^{-1}$ . Although they are ambiguous, the existence of two or more plateaus has supported for other polymers having complex architectures. The calculation data for end-linked star polymer reproduced the plateau region well. In addition to T7, good agreement for plateau regions were seen between the experimental and calculation data for other PPS stars.

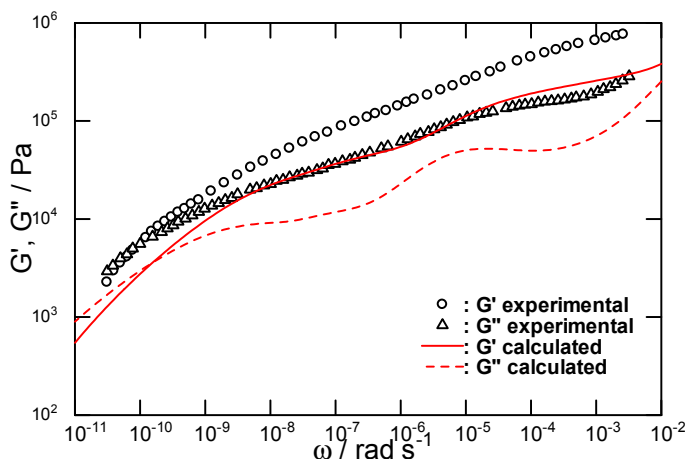


Fig. 21.  $G'$  and  $G''$  for end-linked PPS star (T7) at  $p=0.41$ . ( $p$ : the connectivity extent)

The prediction power of BOB calculation was evidenced by the results shown above for viscoelasticity over wide frequency range. However, the viscoelasticity calculation is presently limited for pre-gel state. It has already found that the calculation values inevitably disagree with  $G'(\omega)$  and  $G''(\omega)$  data of PPS star when  $p$  approaches to the gel point determined by eq.(21). Furthermore, the architecture of the branched polymer becomes complex as the increase in functionalities for  $RA_{fa} + R'B_{fb}$  type reaction, which BOB does not cover with. These are future works toward the comprehensive establishment of the calculation methods for the gelling system.

## 5. Concluding remarks

The rheological method is suitable very much to capture the properties of gel, taking account that rheology is mainly concerned with mechanical properties for substance under deformation. And therefore, research works of a huge number are seen for rheology of sol – gel transition. Of these papers, those related with power law dependences between physical parameters and the variables to control the transition are introduced in Section 2. The phenomenology of the relaxation pattern seems to be completed and is accepted widely. However, little is known yet about the molecular origin of the experimental data of viscoelasticity. Theoretical approach to the power law dependences is expected to help understanding the molecular origin. Such understanding would be desirable from a fundamental point of view.

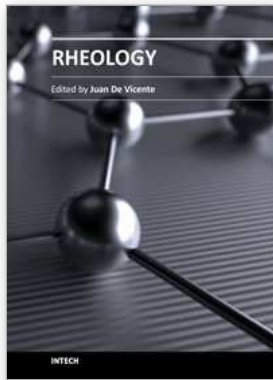
Furthermore, the molecular scheme for the gel point prediction and viscoelasticity calculation in the course of the network formation were described in Section 3 and 4, respectively. Although some simpler models are in demand, the frameworks currently used are too complicated to use conventionally. However, the effect of unequal reactivity on the delay of gel point could be derived by drawing the detailed molecular scheme. Conversely, it is necessary to set the model up to details to meet with the realistic experimental data. Such molecular parameters allows us to prepare materials near the gel point with a wide range of properties for applications, like adhesives, absorbents, vibration dampers, sealants, membranes etc. With suitable design, it will be possible to control network structures, relaxation character, and then mechanical properties to the requirements.

## 6. References

- Ahmad, Z.; Stepto, R.F.T. (1980) Approximate theories of gelation, *Colloid Polym. Sci.*, Vol.258, 663-674.
- Almdal, K.; Dyre, J.; Hvidt, S.; Kramer, O.(1993) Towards a Phenomenological Definition of the Term 'Gel', *Polym. Gels. Networks*, Vol.1, 5-17.
- Brauner, U. (1979) Search for critical exponents at the gel-to-sol transition, *Makromol. Chem.*, Vol.180, 251-253.
- Bromberg, Lev; Temchenko, Marina (1999) Self-Assembly in Aqueous Solutions of Poly (ethylene oxide)-b-poly(propylene oxide)-b-poly(ethylene oxide)-b-poly(vinyl alcohol), *Langmuir*, Vol.15(25), 8633-8639.
- Caillard, R.; Remondetto, G. E.; Subirade, M. (2010) Rheological investigation of soy protein hydrogels induced by Maillard-type reaction, *Food Hydrocol.*, Vol.24(1), 81-87.
- Cates, M. E. (1985) Brownian dynamics of self-similar macromolecules , *Journal de Physique (Paris)*, 46(7), 1059-1077.
- Clark, A. H., Ross-Murphy, S. B. (1987) Structural and mechanical properties of biopolymer gels, *Adv. Polym. Sci.*, Vol.83, pp.57-192
- Das C.; Inkson N. J.; Read D. J.; Kelmanson, M. A.; McLeish, T. C. B. (2006) Computational linear rheology of general branch-on-branch polymers, *J. Rheol.* 50(2), 207-219.
- Das C.; Read D. J.; Kelmanson, M. A.; McLeish, T. C. B. (2006) Dynamic scaling in entangled mean-field gelation polymers, *Phys. Rev. E*. 74, 011404-1 - 011404-10.
- Dušek, K Ilavský, M. Lunňák. S. (1975) Curing of epoxy resins. I. Statistics of curing of diepoxydes with diamines, *J. Polym. Sci. Polym. Symp.*, Vol.53, 29-44.

- Ferry J. D. (1970) Viscoelastic properties of polymers, 2nd ed., Wiley, New York.
- Flory, P. J. (1941) Molecular Size Distribution in Three Dimensional Polymers. I. Gelation., *J. Am. Chem. Soc.*, Vol.63, pp. 3083-3090.; Molecular Size Distribution in Three Dimensional Polymers. II. Trifunctional Branching Units., *ibid.* Vol.63, pp. 3091-3096.; Molecular Size Distribution in Three Dimensional Polymers. III. Tetrafunctional Branching Units., *ibid.* Vol.63, pp. 3096-3100.
- Gordon, M., Ross-Murphy, S. B. (1975) The structure and properties of molecular trees and networks, *Pure Appl. Chem.*, Vol.43, pp.1-26.
- Gordon, M.; Torkington, J. A.(1984) Scrutiny of the critical exponent paradigm as exemplified by gelation, *Pure. Appl. Chem.*, Vol.53, 1461-1478.
- Guenet, J-M. (1992) *Thermoreversible gelation of polymers and biopolymers*, Academic Press, ISBN 0-12-305380-5, London
- Hossain, K. S.; Miyanaga, K.; Maeda, H.; Nemoto, N. (2001) Sol-Gel Transition Behavior of Pure  $\iota$ -Carrageenan in Both Salt-Free and Added Salt States, *Biomacromolecules*, Vol.2(2), 442-449.
- Hsu, Shan Hui; Jamieson, Alexander M. (1990) Viscoelastic behavior at the thermal sol-gel transition of gelatin, *Polymer*, Vol.34(12), 2602-2608.
- Jacobson, H.; Stockmayer, W. H. (1950) Intramolecular Reaction in Polycondensations, *J. Chem. Phys.*, Vol.18, 1600-1606.
- Kjønksen, A. L.; Nyström, B. (1996) Effects of Polymer Concentration and Crosslinking Density on Rheology of Chemically Cross-Linked Poly(vinyl alcohol) near the Gelation Threshold, *Macromolecules* (1996), Vol.29(15), 5215-5222.
- Kjønksen, A.-L.; Nyström, B.; Lindman, B. (1998) Dynamic Viscoelasticity of Gelling and Nongelling Aqueous Mixtures of Ethyl(hydroxyethyl)cellulose and an Ionic Surfactant, *Macromolecules* , Vol.31(6), 1852-1858.
- Koike, A.; Nemot, N.; Watanabe, Y.; Osaki, K. (1996) Dynamic Viscoelasticity and FT-IR Measurements of End-Crosslinking  $\alpha$ ,  $\omega$ -Dihydroxyl Polybutadiene Solutions near the Gel Point in the Gelation Process, *Polym. J.*, Vol.28, 942-950.
- Kwak, S. Y.; Choi, J.; Song, H. J. (2005) Viscoelastic Relaxation and Molecular Mobility of Hyperbranched Poly(E-caprolactone)s in Their Melt State, *Chem. Mater.* Vol.17, 1148 -1156.
- Li, L.; Aoki, Y. (1997) Rheological Images of Poly(vinyl chloride) Gels. 1. The Dependence of Sol-Gel Transition on Concentration, *Macromolecules*, Vol.30, 7835-7841.
- Li, L.; Uchida, H.; Aoki, Y.; Yao, M. L. (1997) Rheological Images of Poly(vinyl chloride) Gels. 2. Divergence of Viscosity and the Scaling Law before the Sol-Gel Transition, *Macromolecules*, Vol.30, 7842-48.
- Muthukumar, M. (1985) Dynamics of polymeric fractals, *J. Chem. Phys.* 83, 3161-3168
- Michon, C.; Cuvelier, G.; Launay, B. (1993) Concentration dependence of the critical viscoelastic properties of gelatin at the gel point, *Rheol. Acta*, Vol. 32(1), 94 - 103.
- Mijovic, J.; Andjelic, S. (1995) A study of reaction kinetics by near-infrared spectroscopy. 1. Comprehensive analysis of a Model Epoxy/Amine System, *Macromolecules*, Vol.28, 2787-2796.
- Miller, D. R., Macosko, C. W. (1978) Average Property Relations for Nonlinear Polymerization with Unequal Reactivity, *Macromolecules*, Vol.11, pp.656-662.
- Nakamura, K.; Harada, K.; Tanaka, Y. (1993) Viscoelastic properties of aqueous gellan solutions: the effects of concentration on gelation, *Food Hydrocolloids*, Vol.7, 435-447.

- Nicol, E.; Nicolai, T.; Durand, D. (2001) Effect of Random End-Linking on the Viscoelastic Relaxation of Entangled Star Polymers, *Macromolecules*, Vol.34, 5205-5214.
- Nicolai, T.; Randrianantoandro, H.; Prochazka, F.; Durand, D. (1997) Viscoelastic relaxation of polyurethane at different stages of the gel formation. 2. Sol-gel transition dynamics, *Macromolecules*, 30(19), 5897-5904.
- Nijenhuis, K. (1997) Thermoreversible Networks, *Adv. Polym. Sci.*, Vol.130, ISBN 3-540-61857-0.
- Peyrelasse, J.; Lamarque, M.; Habas, J.P.; Bounia, N. E. (1996) Rheology of gelatin solutions at the sol-gel transition, *Phys. Rev. E*, Vol.53, 6126-6133.
- Stauffer, D. (1981) Can percolation theory be applied to critical phenomena at gel points., *Pure. Appl. Chem.*, Vol.53, 1479-1487.
- Stepito, R. F. T. (Ed.), (1998) *Polymer Networks - Principles of their Formation Structure and Properties*, Blackie Academic & Professional, ISBN 0-7514-0264-8, London.
- Tan, H.; Moet, A.; Hiltner, A.; Baer, E. (1983) Thermoreversible gelation of atactic polystyrene solutions, *Macromolecules*, Vol.16, 28-34.
- Tan, L.; Liu, S.; Pan, D. (2009) Viscoelastic Behavior of Polyacrylonitrile/Dimethyl Sulfoxide Concentrated Solution during Thermal-Induced Gelation, *J. Phys. Chem. B*, 113(3), 603-609.
- Tanaka, Y. (2009) Viscoelastic Behaviour for End-Linking of Entangled Star Polymer: Application of the Calculation for Branched Polymer to End-Linked Polymer, *Nihon Reorogi Gakkaishi*, Vol.37, 89-95.
- Tanaka, Y.; Xin Yue, J.; Goto, M. (2011) Thermoreversible Sol-Gel Transition of Aqueous solution of Sodium Polyacrylate cross-linked by Aluminium Ions: Derivation of Gel Strength for Aqueous Solution, *Proceedings of 12th IUMRS Int. Confer. Asia*, Taipei, Sep, 2011.
- Truesdell, C.(1945) On a Function Which Occurs in the Theory of the Structure of Polymers, *Annals of Mathematics*, Vol.46, 144-157.
- Valentova, H.; Bouchal, K.; Nedbal, J.; Ilavský, M., (1999) Gelation and dynamic mechanical behavior of liquid crystalline networks, *J. Macromol. Sci., Phys.*, B38(1 & 2), 51-66.
- Vargas, M. A.; Manero, O. (2011) Rheological characterization of the gel point in polymer-modified asphalts, *J. Appl. Polym. Sci.*, Vol.119(4), 2422-2430.
- Vilgis, T. A.; Winter, H. H. (1988) Mechanical selfsimilarity of polymers during chemical gelation, *Colloid Polym. Sci.*, 266, 494-500.
- Winter, H. H. (1987) Evolution of rheology during chemical gelation, *Prog. Colloid Polym. Sci.*, 75, 104-110.
- Winter, H. H.; Mours, M. (1997) Rheology of Polymers Near Liquid-Solid Transitions, *Adv. Polym. Sci.*, Vol.134, 165-234. ISBN 3-540-62713-8.



## **Rheology**

Edited by Dr. Juan De Vicente

ISBN 978-953-51-0187-1

Hard cover, 350 pages

**Publisher** InTech

**Published online** 07, March, 2012

**Published in print edition** March, 2012

This book contains a wealth of useful information on current rheology research. By covering a broad variety of rheology-related topics, this e-book is addressed to a wide spectrum of academic and applied researchers and scientists but it could also prove useful to industry specialists. The subject areas include, polymer gels, food rheology, drilling fluids and liquid crystals among others.

### **How to reference**

In order to correctly reference this scholarly work, feel free to copy and paste the following:

Yutaka Tanaka (2012). Viscoelastic Properties for Sol-Gel Transition, Rheology, Dr. Juan De Vicente (Ed.), ISBN: 978-953-51-0187-1, InTech, Available from: <http://www.intechopen.com/books/rheology/viscoelastic-behaviour-for-gelation>

# **INTECH**

open science | open minds

### **InTech Europe**

University Campus STeP Ri  
Slavka Krautzeka 83/A  
51000 Rijeka, Croatia  
Phone: +385 (51) 770 447  
Fax: +385 (51) 686 166  
[www.intechopen.com](http://www.intechopen.com)

### **InTech China**

Unit 405, Office Block, Hotel Equatorial Shanghai  
No.65, Yan An Road (West), Shanghai, 200040, China  
中国上海市延安西路65号上海国际贵都大饭店办公楼405单元  
Phone: +86-21-62489820  
Fax: +86-21-62489821